Observation of Chain Branching in Polyethylene in the Solid State and Melt via ^{13}C NMR Spectroscopy and Melt NMR Relaxation Time Measurements

M. Pollard, K. Klimke, R. Graf, H. W. Spiess, and M. Wilhelm*

Max Planck Institute for Polymer Research, Postfach 3148, 55021 Mainz, Germany

O. Sperber, C. Piel, and W. Kaminsky*

Institute of Technical and Macromolecular Chemistry, University of Hamburg, Martin-Luther-King Platz 6, 20146 Hamburg, Germany

Received July 1, 2003; Revised Manuscript Received September 17, 2003

ABSTRACT: Branch contents in sparsely short-chain branched polyethylenes ($<C_{28}$) and end-group concentrations in linear polyethylenes were investigated by solid- and melt-state ^{13}C NMR using model copolymers of 1-octene, 1-octadecene, 1-hexacosene, and linear PE standards. Benchmark measurements were established for single-pulse acquisition under MAS on these melts at 423 K, using 7 mm ceramic rotors and commercially available solid-state probes at 300 and 500 MHz ^1H Larmor frequency. Signal improvement by a factor of 3−4 was observed, corresponding to a factor 10 reduction in measurement time, when compared to a reference solution-state (400 MHz ^1H) measurement. Transient NOE effects due to proton decoupling during FID acquisition were found to affect significantly the accuracy of branch content determination and end-group analysis in the melt spectra, even at moderate pulse repetition rates. ^{13}C T_1 and NOE buildup rates and intensity variations were established at 423 K and correlated to the local packing of the branched chain architecture. CP/MAS spectra at and below room temperature on the solid-state polyethylenes showed good agreement with reference spectra, providing an alternative method for sensitivity improvement, with about a factor of 10 saving in measurement time as compared to the melt measurements. Using an optimized parameter set, molecular weight determination of a linear polyethylene standard with M_n>100 000 g/mol was shown to be feasible in both solid-state and melt measurements in less than a one-day measurement, obtained on a 500 MHz spectrometer and 4 mm rotor. Using this enhanced signal intensity, NMR relaxation times were investigated in the melt with respect to their inherent sensitivity to the branching architecture. These measurements included $T_{1\rho}$, T_1, and T_1^{NOE}. It was found that T_1^{NOE} seems to have the best sensitivity to determine the approximate length of the side chain branches for $n > 6$.

Introduction

^{13}C NMR has been established as a versatile tool for elucidating chemical structures and probing local dynamics of synthetic polymers and is widely used in both academic and industrial applications.[1−7] Two classical methods of polymer characterization that continue to benefit immensely from the continuous improvement in ^{13}C NMR methods are end-group analysis and branch-content determination. A particularly interesting case where the capability of ^{13}C NMR is currently being pushed to its limit relates to branch content determination in short- and long-chain branched polyethylenes. Short-chain branched polyethylenes are synthesized by copolymerization of ethylene with one or several alkene-based monomers, which are incorporated into the carbon backbone as side branches typically at concentrations of 1 mol % but might reach up to 19 mol %. The side branches act as structural defects upon crystallization and have considerable effects on crystallization rates, ultimate crystallinity, and solid-state properties, even down to 0.1 mol % comonomer incorporation. In this context, one might think of simple structure−property relationships which are relevant to this class of polymers, such as degree of crystallinity leading to specific solid-state optical properties where short branches (less than 10 carbons) are crucial. Melt elasticity, specifically strain hardening, is influenced by the presence of long branches ($>M_e$, e.g., greater than 300 carbons), even at concentrations of 1 per 10 000 backbone carbons. These play a decisive role in improving or maintaining processability[8] due to the anchoring effect of these entangled side chains.

The historical interest in the properties of branched polyethylenes as studied by ^{13}C NMR spans many decades.[9−29] Recent expansion in this field is primarily due to the successful introduction of new metallocene- and constrained geometry-based catalysts.[30−32] These show improved synthetic control of the final ethylene backbone microstructure and typically eliminate the branching heterogeneity observed in Ziegler−Natta catalyzed polyethylenes. At the simplest level one seeks to correlate the macroscopic properties with the number and size of side branches present along the methylene backbone. But the application of conventional solution-state NMR toward quantitative branch content determination and spectral distinction of branch length continues to be problematic in the case of polyethylene. As discussed extensively in many reviews,[2,4,8] poor sensitivity in combination with vanishing spectral resolution is a major issue. Typical branching signals are a factor of 100−1000 lower in intensity than the predominant signal from the backbone carbons. Other relevant factors include low natural abundance of the detected ^{13}C isotope (1.1%), the long recycle delays required to

* To whom correspondence should be addressed.

10.1021/ma0349130 CCC: $27.50
Published on Web 01/16/2004

maintain signal proportionality (~10 s), the low solubility of PE (~10−20 wt %), broad resonances, and consequently the need to measure at high temperatures (T > 400 K). The detection of long-chain branches in PE is a particularly notable example where any sensitivity improvements would be of great benefit. For branched polyethylenes there are observable enhancements in the zero-shear viscosity starting in the range of 1 long-chain branch per 10 000 CH_2 backbone carbons. In addition to the effect of long-chain branching on processability,[33] there is a further impact of branched structures on the crystallization rates.[34] These two effects account for the high interest given by industry toward branched polyethylenes. The authors of a recent study[27] reported the acquisition of 50 000−2 000 000 transients using high field solution-state NMR (600 MHz, ^{1}H resonance) for a reasonably accurate estimation of long-chain branch contents in the range of 2−10 branches per 10 000 backbone carbons; with 0.5−2.0 s recycle delays, this might correspond to an acquisition time of 1−46 days as calculated from the reported data.[27] Such acquisitions are not likely to be routine or cost-effective.

A potential route to an improved and more efficient measurement of branch percentage using peak integration of ^{13}C spectra is to acquire the signal directly from the neat polymer, either in the solid-state or above the equilibrium melting point. Since polyethylene solution-state spectra are typically conducted around 400 K at no greater than 20 wt % concentrations, one already expects considerable improvements in S/N in the solid state just from the higher filling factor. This direction was initially explored by Hatfield et al.[24] using a 200 MHz spectrometer. The combination of solution-state pulse techniques and solid-state hardware was shown to be a robust method for determining polyethylene branch contents, either by single-pulse excitation in the melt (SPE/MAS) or by cross-polarization in solid-state plugs (CP/MAS). The ^{13}C spectra acquired from the melt showed considerable signal gains over the solution measurement, and additionally the application of MAS reduced line widths to a range encountered in the solution state.

Considering the potential advantage of the solid-state and melt-based methods, they appear to have made little impact so far on routine branch content determination or end-group analysis. If the solid-state spectra were calibrated against melt and solution-state measurements, then one might be able to extend the current sensitivity limit of NMR to determine branch contents, particularly with respect to sparse long-chain branch content. A room temperature measurement using cross-polarization, for instance, would already improve the situation further due to the higher initial proton polarization, giving an expected improvement in sensitivity by up to ~4 and therefore in measurement time by ~16. Additionally, the relaxation delay would only be limited by the much faster proton relaxation (typically 1−3 s) compared to the relaxation time of the carbons (typically 10−100 s).

With this goal in mind, we have studied how to improve the melt and solid-state NMR approaches to improve measurement efficiency while maintaining a degree of quantifiability. We have placed emphasis on the optimization of experimental conditions and acquisition parameters, which are expected to have an impact on the analysis of both the short- and long-chain types found in polyethylenes. A selection of several lab-grade branched polyethylenes were chosen as model short-chain branched systems, and the consistency between the solution, melt, and solid-state NMR measurements was examined. These model systems should provide us first with defined polymer structures and second the possibility to fully optimize the solid-state NMR technique for later application toward more complex and industrially relevant systems. An important goal at the outset was to establish the current sensitivity limits of these techniques as measured under optimal conditions, even though at still fairly moderate field strength (300 and 500 MHz ^{1}H resonance), as they pertain to branch content determination and end-group analysis in polyethylene.

Our work extends the groundwork laid by Hatfield in the following ways: (1) reduction of the comonomer content by a factor of 10 using specifically synthesized model systems; (2) use of lower temperature (423 K instead of 473 K) for SPE, thereby reducing impact of decomposition and reducing spin−lattice relaxation times; (3) the use of a fully digital spectrometer at higher B_0 field, with systematic optimization of experimental parameters; (4) use of higher decoupling strength (CP/MAS) for line width reduction and low temperatures (253 K) to freeze out dynamic heterogeneities; (5) examination of transient NOEs on signal intensities of both side-chain branch carbons and end-group carbons in the melt; (6) selection of model linear PEs for M_n detection via solid-state NMR and comparison with GPC; and (7) investigation of relaxation time parameters (T_1, T_1^{NOE}, and $T_{1\rho}$) toward their usage for SCB detection for n > 6.

Extending the sensitivity of NMR toward varying branch lengths, however, will require a different approach. Since the chemical shift is related primarily to electronic shielding, there will be a decreasing contribution to the local field at a given branch carbon nucleus as the branch length is increased. For example, one finds that the methine carbon at the backbone-branch junction point shows an absorption resonance at 38.283 ppm for an n = 6 branch, 38.286 ppm for an n = 8 branch, and 38.293 for an n = 10 branch, when measured at the highest resolution currently available (188 MHz ^{13}C, or 750 MHz ^{1}H).[26] This trend must ultimately reach a plateau that depends on the instrument's resolving power, thus eliminating all chemical shift resolution. Even with further increases in magnetic field strength, it is unlikely that improvements in resolution (via the applied B_0 field) would ever allow the distinction of n = 20 branches from n = 40 branches, for instance. Branches longer than n = 10 are thus "long" in the spectroscopic sense (at the more widely available 300 MHz ^{1}H frequency, the limit is about n = 6), while a long branch is only active in a rheological sense for branches longer than n = 300 or so. The gray area defined by these two limits 6 < n < 300 presents an unresolved experimental problem: how to spectroscopically distinguish short and long branches. Both types need to be present in some degree to provide both processability and ultimate property control.

The length of the branches, however, also affects the local segmental mobility. Therefore, our second goal was to specifically explore those aspects of the local dynamics that could offer improved sensitivity to side branches longer than n = 10. Relaxation time parameters (e.g., T_1, T_2, or $T_{1\rho}$ for carbons) might be able to distinguish branch lengths in cases where chemical shift invariance

Table 1. Molecular Characteristics of Linear and Branched Polyethylenes

polymer	label	M_w (kg/mol)	M_n (kg/mol)	T_m (°C)
linear, oligomer	C-44	0.618	0.6	140
linear	L-12	16.5	12	140
linear	L-60	91.5	60	140
linear	L-110	181	114	140
branched, 1-butene	B-2			
branched, 1-octene	B-6a	179		122
branched, 1-octene	B-6b	135		116
branched, 1-octene	B-6c	130		110
branched, 1-octadecene	B-16a	160		120
branched, 1-octadecene	B-16b	129		116
branched, 1-octadecene	B-16c	93		110
branched, 1-hexacosane (C-26/28)	B-26a	112		122

has already set in. The underlying idea is that the local melt dynamics should be directly influenced by the defects caused by the branched structure, which affects the local molecular packing. NMR relaxation parameters are very sensitive toward changes in local dynamics due to the combined influence of the spectral density of the fluctuations and the $\langle r^{-6}\rangle$ dependence of the dipolar quenching by mobile protons. In general, previous studies have shown that the ^{13}C T_1s of carbons along short side branches (e.g., the methyl carbon) increase linearly as the branch length increases, while the carbons along the backbone near the branch (e.g., the methine, α, and β carbons) show decreasing T_1s with branch length, in both the melt and solution state. These trends are traced to the restriction of local megahertz motions in the vicinity of the branch points by the branch point itself. The perturbations of these motions can be clearly observed in the ^{13}C relaxation characteristics.[35,36] Within this article these empirical correlations were extended to branch lengths beyond $n = 10$, using model branched polyethylenes to quantify relaxation parameters.

Experimental Section

Narrow molecular weight distribution polyethylenes were obtained from several sources. The molecular characteristics of the investigated linear and short-chain branched polyethylenes are summarized in Table 1. 1-Octene and 1-octadecene copolymers, denoted B-6 and B-16, were synthesized using a constrained geometry ansa-metallocene catalyst, [Ph_2C(di-*tert*-ButFlu)(Cp)]$ZrCl_2$, under conditions producing sparse branches from the copolymerization of ethylene and the chosen 1-alkene.[30] Longer side branches were synthesized using an α-olefin mixture purchased from CPchem, consisting of 50−62% C_{26} and 30−42% C_{28} content. These higher olefin copolymers are denoted B-26. Branch contents were determined using the NMR analysis described below. The NMR spectroscopically detected average branch density is reported in Tables 2 and 4 as the average number of branches per 1000 backbone carbons. Using this definition, 1 branch per 1000 carbons equals approximately 0.2 mol % alkene comonomer content. For the determination of the M_n of the linear PEs, the chain end methyl signal and the methylene signal were used for integration. In addition, several linear standard polyethylenes were purchased from Polymer Standards Service, Mainz, Germany, in order to provide a reference M_n for end-group analysis and to calibrate the NMR results with respect to the GPC data.

^{13}C NMR melt and solid-state measurements were performed on either a Bruker DSX-300 (75 MHz ^{13}C Larmor frequency) or a Bruker DSX-500 (125 MHz ^{13}C Larmor frequency). For the DSX-300, we used a commercially available high-temperature MAS probe (7 mm rotors), and for the DSX-500 we used standard MAS probes (4 and 7 mm rotors). Unless otherwise indicated, 100−200 mg of unmodified PE powder was packed into the MAS rotors and secured with a high-temperature BN cap. In several cases we used a melt press to increase even further the filling factor of the rotor (up to 50% increase). The rotors were bathed in N_2 bearing gas to prevent oxidative degradation and radical combination. Direct heating of the bearing gas provided a temperature stability of the exit gas of ±0.1 °C during MAS. Chemical shift values were calibrated using adamantane as external reference at room temperature. The 90° pulse lengths were between 4 and 10 μs, determined directly on the neat PE melts under measurement conditions. The melt measurements employed digital filtering and oversampling; the actual sampling interval was 2.5 μs (12× oversampling at a nominal dwell time of 30 μs). It is important to note that the dynamic range of the ADC might limit the possibility to detect sparse branching. A 16 bit ADC is highly recommended, where in the case of an actual experiment only 15 bits might be used. If a CH_3 signal is digitized using only 2 bits, then a signal of 2^{13} times higher such as the bulk methylene signal, CH_2, can still be analyzed. For a linear PE, this would translate to an upper detectable limit for M_n of about 230 000 g/mol.

For MAS measurement at room temperature and below, rotors were either packed with powder (∼200 mg) using a flat pressing tool to provide an even sample distribution or filled with a PE plug (∼300 mg) prepared using a melt-press. However, the latter were more susceptible to spinning instability at room temperature due to the presence of encapsulated air bubbles. For MAS measurement at high temperatures (above T_m), we found that the hardware of the MAS probe can be easily damaged by unbalanced rotors due to initial sample packing; the stator was particularly vulnerable to damage while heating the rotor in situ. To begin an experiment at high temperatures under MAS, we found that it was best first to fill the rotor with PE powder or a plug and spin the rotor at 0.8 kHz or less; the bearing and drive gas flow rates must be set manually. The temperature can then be increased incrementally until the melting point is reached (∼140 °C) while maintaining the bearing and drive gases at a constant value. As the sample melts and centrifugates above T_m, spinning stability improves. This is generally indicated by an increasing spinning rate if the gas flow rates are held constant. It is important not to increase the spinning rate beyond 1 kHz unless it is certain this state of flow is being achieved. This required no more than several minutes for the polyethylenes having $M_n \sim 100\,000$ g/mol used this study but will require increasingly longer times for higher molecular weights. The spinning speed may then be increased to the desired rate (∼3 kHz) and the automatic control of the bearing and drive gases activated. If the molten PEs will not spin above 1 kHz, this can be attributed to either dirt in the sample (residual catalyst particles, etc.) or perhaps cross-linking which might hinder flow, and generally the experiment must be halted. We found that rotors packed with PE plugs which do not centrifugate above their melting point are the most susceptible to cause rapid stator damage, sometimes with no indication of spinning instability.

Sample removal after MAS measurement was easily achieved for the samples in this study. For high-temperature MAS, slow cooling of the rotor below T_m while spinning always preserved the cylindrical shape of the sample; thin opaque cylinders of PE could be quickly removed from the rotor by quenching in liquid nitrogen. In rare cases where sample degradation/cross-linking was a factor the sample became glued to the rotor; in this case, a drill was used to excavate the bulk of the sample, but aggressive solvents were never required.

Solution-state measurements were performed on a Bruker Avance-400 (100 MHz ^{13}C Larmor frequency) at 373 K with perchlorobutadiene (PCB) and 1,1,2,2-tetrachloro-1,2-dideuterioethane (TCE) as solvents. Liquid-state ^{13}C spectra were acquired with inverse-gated decoupling, 30° pulse angle, 10 s recycle delay, and 4096 scans per spectra. Sample concentration was ∼10 wt % in 10 mm glass vials.

Branch content was determined by numerical peak integration of branching signals from the melt ^{13}C SPE/MAS spectra taken at 423 K, with 3 kHz MAS frequency and dipolar

decoupling (25 kHz). It was experimentally found that above a dipolar decoupling field strength of 25 kHz the reduction in line width for the melt leveled off. Typical acquisition parameters were >128 scans per spectrum, 4 μs 90° pulse length, 122 ms acquisition time, dwell time of 30−40 μs, 4K data points, and zero filling to at least twice that number. Exponential line broadening at the matched filter condition (5−10 Hz) was applied for optimum signal-to-noise improvement. The recycle delay varied for the melt between 2 and 60 s. The magnetization tip angle was likewise optimized to be 90° (≠ Ernst angle) as will be discussed below.

CP/MAS spectra were obtained with reduced acquisition times of 40−60 ms, increased dipolar decoupling (≈50 kHz), and recycle delays of typically 2−5 s. The limit for the recycle delay is caused by the long acquisition times and consequently hardware constraints due to the limited duty cycle of the spectrometer. Rotor frequencies have been tested for CP measurements and were found to be optimum around 3 kHz as a compromise of line width and magnetization transfer rate T_{CH}. Using this rotor frequency, the overlap between spinning sidebands of the dominant CH_2 resonance and the CH_3 resonance was avoided.

The ^{13}C T_1s were determined at 423 K via an inversion recovery pulse sequence (180°−τ−90°) with variable delay time τ, MAS at 3 kHz, and dipolar decoupling during acquisition. General acquisition parameters were 4 μs 90° pulse width and 122 ms acquisition time. For the detection of carbons close to the CH group along the backbone (α and β carbons, see Figure 2), specific parameters were 264 scans per spectrum, 4 s recycle delay, and at least six delay times τ such that 0.1 s < τ < 2.5 s. For the branch carbon observation at the side chain, specific parameters were 64 scans per spectrum, 60 s recycle delay, and at least six delay times τ such that 1 s < τ < 60 s. The drastically longer recycle delay for the detection of the side chain branches was caused by the longer T_1 of these carbons. Signal intensities showed exponential recovery and were fit to $M(\tau) = M_i + (M_i - M_\infty)[1 - \exp(-\tau/T_1)]$, to a minimum in χ^2. Error bars in T_1 are reported as the 95% confidence level of the time constant determined by the fit, shown only as an indication of the quality of fit. Comparison of several data sets taken with a different set of delay times showed a maximum difference of 10% in the relative detected value. We expect 10% relative error for independent measurements of T_1 at 423 K in branched polyethylenes.

NOE buildup curves were determined by applying a pulse train on ^1H $(90°-\tau_{rec})_k$ with variable k, followed by a 90° sampling pulse on ^{13}C, observed with MAS of 3 kHz and dipolar decoupling. The 90° ^1H pulse width was 4 μs, τ_{rec} was 4 ms, and k varied from 1 to 5000. The recycle delay was 60 s for observing branch carbons and 10 s for backbone carbons. Signal intensities showed an exponential increase from initial magnetization to a terminal value as a function of (kt_{rec}) and were fit to the equation $M(n\tau_{rec}) = M_i + \eta[1 - \exp(-n\tau_{rec}/T_1^{NOE})]$, where the NOE factor is defined as $\eta = M_\infty/M_i$.

^{13}C $T_{1\rho}$s were determined in the melt at 423 K under a spin-lock field equivalent to 25 kHz B_1 field strength for variable times τ, with MAS of 3 kHz and dipolar decoupling during acquisition. Branch carbon signals showed no signal decay during the maximum 120 ms spin-lock time. This maximum value is a result of hardware limitations for the applied strong lock fields. Backbone carbon intensities under spin-lock conditions showed exponential decays and were fit to $M(\tau) = M_i \exp(-\tau/T_{1\rho})$.

Results and Discussion

Single-Pulse/MAS in the Melt. Two ^{13}C spectra obtained from sample B-6c are shown in Figure 1. The solution-state spectrum obtained at 373 K is shown in (a), and the MAS spectrum obtained at 423 K in the melt is shown in (b). The spectra are for convenience normalized so that the standard deviation of the noise is identically 1 and displayed on equivalent scales. The branching peaks can be identified using the schematic diagram and notation of Figure 2. Greek letters denote "backbone" carbons which lie at increasing distance from the branch point, and numerals indicate the position of a "branch" carbon relative to the methyl group, which is labeled 1. The two spectra shown in Figure 1 were obtained on the same copolymer under nearly identical conditions, and both represent a typical overnight measurement (10−15 h). See Table 2 for a list of the relevant acquisition parameters.

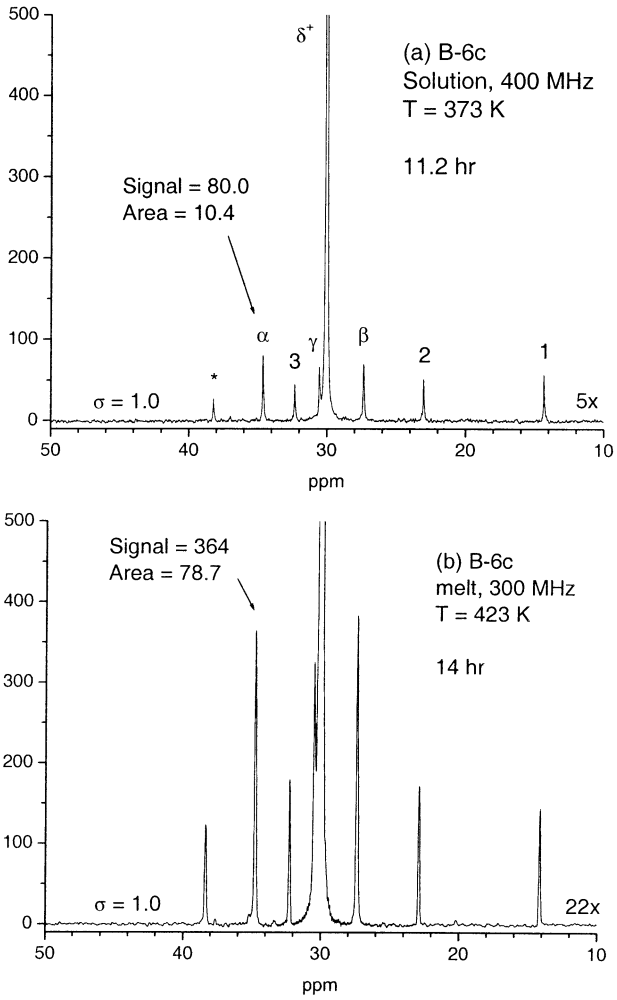

Figure 1. ^{13}C spectra of sample B-6c in the (a) solution state at 373 K and (b) SPE/MAS melt state at 423 K. See Table 2 for a summary of relevant parameters. Spectra are normalized to a similar noise level, and peak intensities and areas for the α carbon are indicated.

Table 2. Summary of Relevant Parameters for the Spectra Shown in Figure 1

Figure	1a	1b
sample	B-6c, solution	B-6c, melt
pulse seq	SPE	SPE/MAS
instrument (MHz)	400	300
T (K)	373	423
no. of transients	4096	5600
rec delay (s)	10	9
S/N	80	364
time (h)	11.3	14
branches/1000	9.7	11.6

The sensitivity improvement due to the higher filling factor of the undiluted melt can be estimated by comparing the signal areas of the α carbon resonance at 34.6 ppm. This peak is used as an internal sensitivity reference. Comparison of the two α signals shows that the melt measurement offers factor of 8 increase in area,

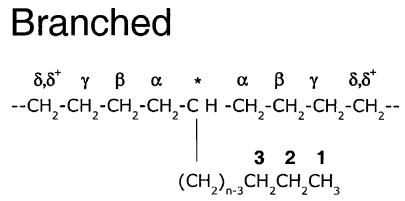

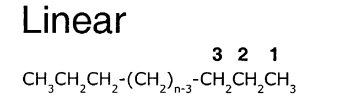

Length of Branch

	2	4	6	8	10
*	39.79	38.243	38.283	38.286	38.293
α	34.145	34.626	34.639	34.646	34.653
β	27.357	27.334	27.343	27.351	27.355
γ	30.491	30.491	30.5	30.505	30.508
δ	30	30	30	30	30
1	11.158	14.046	14.02	14.018	14.015
2	--	23.367	22.881	22.864	22.852
3	--	29.573	32.213	32.195	32.184
4	--	--	--	29.591	29.574
5	--	--	--	29.935	29.925

Figure 2. Schematic diagram showing the applied nomenclature. The table of chemical shift values shown here, previously determined on polyethylenes in the solution state,[26] were used to identify backbone and branch carbons.

clearly a significant improvement in measurement efficiency (a factor of 64 in time) over the solution state. Notably, the melt offers this sensitivity improvement despite an increased line width ($fwhm_{\alpha,melt} \approx 1.3$ ppm, $fwhm_{\alpha,soln} \approx 0.7$ ppm). Peaks were found to display Lorentzian shapes. It is additionally surprising to observe this improvement even though the sample mass (~200 mg) was roughly the same for both the solution-state vials and the solid/melt-state rotors. Throughout the investigation we observed a factor of ~8 overall improvement in the melt spectra when referenced to the solution state, using a melt recycle delay of 10 s (to be optimized, see below) and applying a lower field strength. This corresponds to roughly a factor 50−100 reduction in measurement time, depending on the sample. Clearly, it is this factor which can be exploited to provide increased sensitivity in the determination of sparse branch contents.

The sensitivity limits of the melt MAS toward end-group analysis was investigated using two linear standard polyethylenes, denoted L-12 (M_n = 12 000 g/mol) and L-60 (60 000 g/mol). The melt ^{13}C/MAS spectra of these two linear standards obtained at 423 K are displayed in Figure 3, with acquisition parameters listed in Table 3. The resonances from carbons 1, 2, and 3 are unique identifiers of the chain ends and can be used for quantifying the molecular weight by determining their relative areas with respect to the bulk methylene resonance at 30.0 ppm. Because of the rapid (~terahertz) 3-fold reorientation of the two methyl groups at the chain ends at 423 K, the initial assumption was that these methyl and nearby carbons would have extremely long T_1s. (There are no reports in the literature of the ^{13}C T_1s of these carbons at a linear chain end.) Since quantifying the carbon signals requires a recycle delay time between FID acquisitions of ~5× the longest ^{13}C T_1 to ensure full relaxation of all carbon polarization between pulses, a conservative 60 s recycle delay was

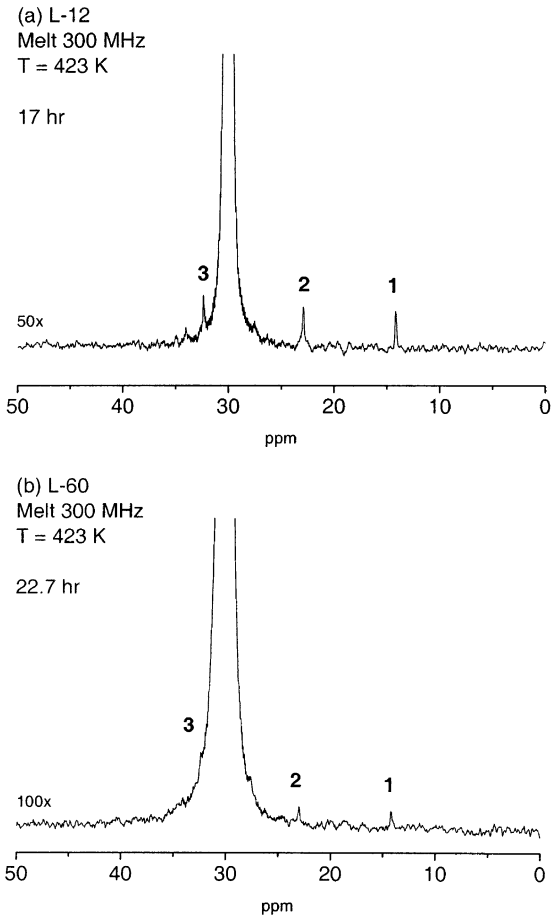

Figure 3. ^{13}C SPE/MAS spectra obtained at 423 K for (a) linear PE, M_n = 12 000 g/mol, and (b) linear PE, M_n = 60 000 g/mol, measured in less than 1 day. See Table 3 for a summary of relevant parameters. The spectra are quantitative and show no major indication of any additional branched structure besides the linear one.

Table 3. Summary of Relevant Parameters for the Spectra Shown in Figures 3 and 8

Figure	3a	3b	8a	8b
sample	L-12	L-60	L-110	L-110
pulse seq	SPE/MAS	SPE/MAS	SPE/MAS	CP/MAS
instrument (MHz)	300	300	500	500
T (K)	423	423	423 ± 10	253
no. of transients	1024	8192	30000	30000
rec delay (s)	60	10	2	2
S/N	8.4	3.7	3.6	7.9
time (h)	17.1	22.7	16.7	16.7
end groups/1000	2.3	0.46	0.24	0.24
NMR M_n (kg/mol)	13.9	64.5	122.8[a]	134.4
GPC M_n reference	12.0	60.0	114.0	114.0

[a] Determined from an average of carbon 2 and 3 resonances.

chosen for sample L-12. In a 17 h acquisition, the end groups displayed a signal-to-noise of 9, with M_n determined at 13 900 g/mol (GPC reference M_n = 12 000 g/mol). For the higher molecular weight standard, L-60, a shorter recycle delay of 10 s was chosen; after 22 h acquisition, the end groups displayed a signal-to-noise of 4, with M_n determined at 64 500 g/mol (GPC reference M_n = 60 000 g/mol). A relative error of 15% compared to GPC data was therefore observed in both cases (see Table 3), showing that end-group determination was feasible up to M_n = 60 000 g/mol in a 1 day acquisition.

We have used the signal-to-noise of the methylene resonance, $(S/N)_{\delta+}$, from the linear and branched polyethylenes in this study to establish a benchmark for our particular instrument configuration (7 mm ceramic

rotor, solid-state high-temperature MAS probehead, DSX-300) and experimental conditions (~200 mg PE, $T = 423$ K (melt), $\omega_{rotor}/2\pi = 3$ kHz MAS, single-pulse experiment with dipolar decoupling). When plotted on log scales, $(S/N)_{\delta+}$ was linearly proportional to the number of scans acquired, NS, with a best fit to the equation: $\log(S/N)_{\delta+} = 1.86 + 0.46 \log(NS)$. This is the expected $S \sim (NS)^{1/2}$ scaling for co-addition of FID transients. This benchmark will provide a useful reference to compare melt spectra obtained on higher field instruments, with the use of smaller diameter rotors, especially optimized $^1H-^{13}C$ probes, or the further addition of relaxation agents (e.g., $Cr(AcAc)_3$).

From this fit, an explicit prediction can be immediately made regarding the absolute sensitivity limit of melt NMR toward branch content and end-group analysis in polyethylene. However, two time-based constraints must first be established in order to define this sensitivity limit: (1) the choice of recycle delay time, as this controls how rapidly FIDs may be acquired and co-added, and (2) an agreed-upon minimum S/N observed at the branching signal (e.g., α resonance) or end-group signal (e.g., methyl), as this value controls how many transients must be acquired and co-added for a sufficient estimate of signal area above the surrounding noise. These two parameters are chosen at the outset of an experimental acquisition and specify respectively the rate at which signal accumulates and the time at which the experiment is halted.

In branch content determination, we will initially assume that 10 s is a sufficiently long recycle delay ($>5T_1$) between pulses to allow full relaxation of the two carbon peaks used for integration: the bulk carbon ($T_{1,\delta+} \approx 1.5$ s) and the carbons α to the branch point ($T_{1,\alpha} \approx 0.5$ s). We further assume that the signal-to-noise of the α carbon resonance be at least 10, $(S/N)_{\alpha,min} = 10$, which should provide a relative accuracy of 10% on the peak area by integration. For experiments performed under these constraints, we estimate that the branch content can be determined down to a concentration of 1 branch per 1000 backbone carbons in a matter of ~1 h using a 300 MHz instrument. This value was computed using the fit above, assuming that the α peak is used for integration.

This estimate is supported by the spectrum shown in Figure 1b, which was acquired under similar constraints, as can be shown by a simple scaling argument using $S \sim (NS)^{1/2}$ and the relevant acquisition data ($(S/N)_\alpha = 364{:}1$ for sample B-6c, a 1-octene copolymer with a branch content of ~10 per 1000 backbone carbons, obtained with 9 s recycle delay). Stated differently, less than 1 h was actually needed in this case to fully quantify the branch content, to a S/N = 10 level, and the additional measurement time simply improved S/N without substantial benefit.

Arguing further along these lines, we estimate that the sensitivity limit expected for a 1 day measurement (24 h) will be improved by a factor of $(24)^{1/2} \approx 5$, bringing the "sparse" branch range of 2 per 10 000 backbone carbons within reach. Although short-chain branched polyethylenes will have a limited impact on the bulk physical properties when present at this concentration, any medium- or long-chain branches will dominate the terminal melt mechanical relaxation behavior and melt elasticity but might be below detection limits for other analytical techniques, such as GPC, light scattering, and dilute solution viscometry.

A similar argument can be made for the sensitivity limit to quantify end groups in polyethylene. Using the results above, we estimate that it will require 24 h measurement time for molecular weight determination of a linear polyethylene of $M_n = 15\,000$ g/mol, again under the accepted constraints of a 10 s recycle delay measured to S/N = 10 on the end methyl carbon. Clearly, the determination of commercially relevant chain lengths will require a sacrifice of S/N and/or an increase in the pulse repetition rate. This is supported again by the results obtained on the linear standard with $M_n = 60\,000$ g/mol shown in Figure 3. Here, the acquisition was halted at 22 h, thus giving only S/N = 4 on the methyl carbon.

In this range of detection of sparse end groups or branches, further improvements in sensitivity can be obtained by relaxing the two time constraints discussed above, but doing so will have unavoidable side effects. Measuring to a lower S/N, i.e., settling for a noisier measurement as in Figure 3b, is the less favorable option, but fitting of spectral resonance lines to a Lorentzian line shape will partially offset this problem. A more reliable technique is to reduce the recycle delay provided that the inevitable steady-state effects on the signal intensities can be accounted for. Such rapid pulsing on an unrelaxed spin system can generate well-known intensity distortions. To extend the sensitivity limits of melt ^{13}C NMR as far as possible, we have extensively studied these steady-state effects in both branched polyethylenes and the linear standards. We discuss these results below, first in the context of end-group analysis and then with a branched 1-octene copolymer.

Steady-State Effects. To extend the sensitivity further and bring commercially relevant polyethylenes ($M_n > 100\,000$ g/mol, or 1 branch per 10 000 backbone carbons) within reach, one must pulse as rapidly as possible within the limits of the available solid-state hardware. Furthermore, any steady-state effects on the signal intensities should be clearly understood in order to interpret the results with a degree of confidence. We chose to study these effects systematically using a monodisperse oligo-ethylene ($M_n = 618$ g/mol, $M_w/M_n = 1$) as a model compound for a longer chain. This provided sufficient signal intensities to study in detail the relaxation and steady-state effects, which required the acquisition of multiple data sets within a time window usually limited by sample degradation (~1 day). The ^{13}C T_1s were first determined by inversion recovery at 423 K in the melt. The data are shown in Figure 4a. The four resolvable carbons showed a dispersion in their spin−lattice relaxation times: $T_{1,C1} = 14$ s, $T_{1,C2} = 12$ s, $T_{1,C3} = 9$ s, and $T_{1,bulk} = 3$ s. This indicates that significant saturation of the carbons near the chain end will be observed in the single-pulse acquisitions for any recycle delay less than 30 s, and generally a fully quantitative experiment will require 60 s between successive pulses for full relaxation.

To examine the effect of saturation on the observed signal intensities, a series of spectra were acquired with a progressively reduced recycle delay, RD. At RD = 60 s, a chain length of $n = 46$ ($M_n = 646$ g/mol) was determined by integration, in excellent agreement with the expected chain length of $n = 44$ ($M_n = 618$ g/mol), a relative error of 5%. As shown in Figure 4c, unexpected oscillation in the signal intensities was observed at lower recycle delays. One expects in general that the

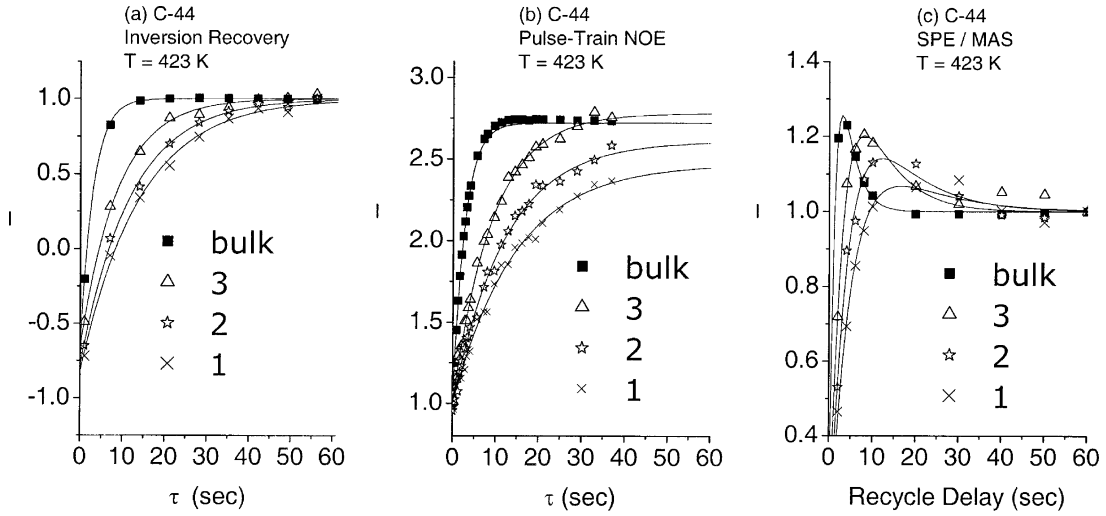

Figure 4. Results of (a) inversion recovery and (b) transient NOE measurements on the oligo-ethylene C-44 at 423 K (melt). (c) displays the total intensity distortions observed in the single-pulse experiment as a function of the recycle delay. At short recycle delays, corresponding with a strong reduction in measurement time, an increase in signal of up to 25% is observed.

signals will saturate at low recycle delays and therefore be accompanied by a reduced signal intensity, as given by the relevant ^{13}C T_1s. Here, however, a signal increase is observed for 10 s < RD < 60 s, while a signal decrease is observed for RD < 10 s.

Such effects have been observed previously in single-pulse acquisitions in the solution and solid-state in at least two cases[28,37] and were traced to a transient nuclear Overhauser enhancement (NOE) arising from the high-power proton decoupling during FID acquisition. The effect is understood as follows: if the high-power proton decoupling is followed too rapidly by the following observe period, such that proton polarization has not fully relaxed before the next carbon pulse, then NOE enhancements at the carbons can be observed. As a result, the signal intensities show a complex dependence on the recycle delay, as shown in Figure 4c. The signal intensities can be described by the following equation:[28]

$$I(t)/I_{eq}(t) = 1 + (\eta/A)\exp(-t/T_{1,H}) - (1 + (\eta/A))\exp(-t/T_{1,C}) \quad (1)$$

where $A = 1 - T_{1C}/T_{1H}$ and η is the steady-state NOE factor. Whether a given carbon signal is enhanced or reduced depends on the relative values of the ^{13}C T_1s, the ^{1}H T_1s, and the steady-state NOE factors of each carbon site.

To check the consistency of this equation with our results on the oligo-ethylene, we independently determined the ^{13}C spin−lattice relaxation times (see Figure 4a) and NOE buildup curves by pulse-train NOE measurements (see Figure 4b) at 423 K. The intensity data were then fit using eq 1, with the ^{1}H T_1 left as a floating parameter. The best fits obtained using this procedure are displayed in Figure 4c and reproduce the qualitative features of the data well. The results of the fitting procedure show also that the hydrogens attached to bulk carbons should display the fastest proton relaxation time (best fit to 1.4 s) while the hydrogens near the chain end should display slower relaxations (best fit to 3.9, 4.4, and 4.1 s for carbons 3, 2, and 1, respectively). However, independent experimental evidence of a dependence of the ^{1}H T_1 on either the chain length or side-branch length (see below) was difficult to demonstrate because of the inherently broad (overlapping) proton lines encountered in the melt state and possible nonexponential character of the proton relaxation. Equation 1 therefore provides only an approximate description of the impact of the steady-state NOEs on intensities, but at least demonstrates that the curve shape in Figure 4c is caused by the residual proton polarization from decoupling.

The effects on signal intensities must be regarded as highly sensitive to the local mobility, which is reflected in the three parameters in the equation above. However, there are some limits on the possible values these parameters can adopt, at least in the highly mobile system studied here. In polyethylenes, the NOE is in general fully developed for carbons (∼3); i.e., dipolar relaxation dominates the carbon relaxation. Further, we observed proton relaxation times within the range of 1.5−3 s at 423 K in all the linear PEs and copolymers studied here. The major distinction in how signal intensities react to the rapid pulsing thus appears to be controlled only by the carbon relaxation times, which range from 0.5 to ∼15 s.

We have also studied the transient NOE effect on the octene copolymer, sample B-6b, anticipating that similar effects would be observed. The experimentally observed distortions in signal were more severe in this case because of a wider disparity in the ^{13}C T_1s among the carbons near the branch point. In Figure 5 the absolute signal intensities of all spectrally resolved carbons are shown for sample B-6b as a function of the recycle delay. While the backbone carbons (Figure 5a−c) show signal enhancement as the recycle delay is reduced, the carbons at the side chain ends (Figure 5d) show a reduction in intensity. The ^{13}C T_1s of sample B-6c were measured at 423 K by inversion recovery and are summarized in Table 5. The backbone carbons near the branch point display the fastest relaxation (∼1 s) while the end branch carbons display the slowest relaxation (∼10 s).

The transient NOE thus affects branch content determination most severely if the end groups of the side-chain branch carbons are used to compare peak integrals. This was very clearly observed from the results of numerical integration of the spectral lines, as shown

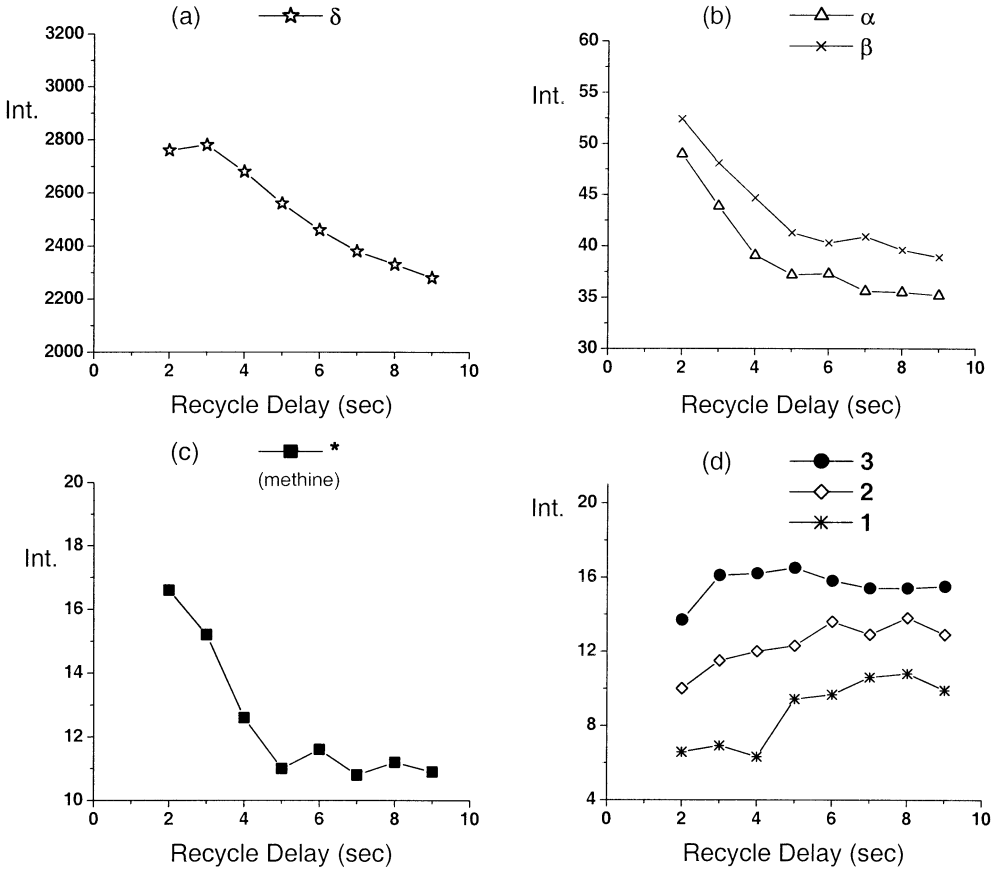

Figure 5. Effect of progressive reduction of the recycle delay in the ^{13}C/MAS spectral intensities in the sample B-6b at 423 K, as observed in the absolute signal intensities of (a) ∂ carbon at 30.0 ppm, (b) α and β carbons, (c) methine carbon at branch point, and (d) carbons 1−3 alongside branch.

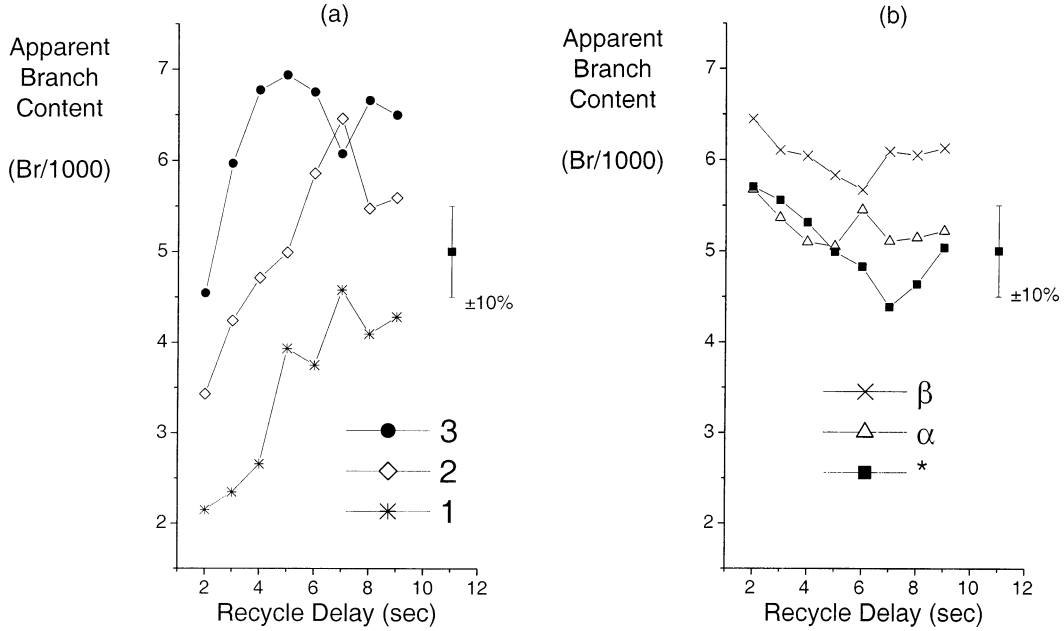

Figure 6. Apparent branch contents determined by peak integration for sample B-6b at 423 K, determined as a function of the recycle delay. Results are shown for peak ratios of (a) side branch carbons and (b) backbone carbons near the branch point. The ratio for the main resonance with respect to the α and β carbon is clearly preferential due to the lower error.

in Figure 6. The apparent branch content was determined by comparing the bulk methylene peak area with either the branch carbons (Figure 6a) or the backbone carbons (Figure 6b). 10% error bars are shown as a guideline for the expected accuracy. From these data, one could easily under- or overestimate the branch content by 50% by using the end groups of the side-chain carbons. The backbone carbons offer the best reproducibility, however, even down to a 2 s recycle delay.

One strategy often employed in solution-state acquisitions to circumvent or minimize saturation effects, and improve sensitivity, is to select a lower pulse angle (i.e., the Ernst angle). To investigate whether this approach would eliminate or modify the transient NOE, we

examined the effect of pulse angle on the signal intensities under rapid pulsing. At progressively lower recycle delays, the relative intensities showed the same behavior as in Figure 5 for pulse angles of 90°, 45°, and 30°. Choosing lower pulse angles therefore simply reduced the signal intensity with no effect on the transient NOE and with no sensitivity benefit. The optimum pulse angle therefore appears to be 90° for single-pulse acquisitions when the transient NOE dominates signal intensity.

We additionally studied the effect of the applied decoupling power and the total acquisition length (i.e., the total decoupling time) on the signal intensities under rapid pulsing. For applied ^{1}H decoupling strengths of 3−42 kHz (measured with FID length of 120 ms) and for FID lengths of 15−120 ms (measured at decoupling strength of 25 kHz), the bulk methylene signal displayed no observable deviations from the curves as shown in Figure 5. The line width was constant at a decoupling strength above ∼25 kHz. These observations add further support to the description of this effect based on eq 1: in the single-pulse experiment, the transient NOEs are not controlled by any choice of acquisition parameters, but by the local motional characteristics reflected in the ^{1}H and ^{13}C T_1s. One therefore expects to encounter this phenomenon to some degree whenever applying ^{13}C single-pulse acquisitions on neat polyolefin melts.

Although the signal proportionality is lost for any RD < 10 s, some signal ratios remain a proportionate quantity down to RD = 2 s, i.e., S_*/S_δ, S_α/S_δ, and S_β/S_δ. From a time standpoint, then, one might choose a 2 s recycle delay in order to improve sensitivity for branch content determination by $(5)^{1/2}$ as long as this caveat is kept in mind. This is an improvement on our previous estimate of the absolute sensitivity limit in the determination of branch contents. To a S/N = 10 level, using RD = 2 s, the sensitivity limit by melt ^{13}C NMR is 2 branch in 10 000 backbone carbons in a 1 day measurement, if observed at the α carbon.

CP/MAS in the Solid State. One motivation to extend branch content determinations into the solid-state PE is to reduce the extensive recycle delays and improve sensitivity via extensive signal averaging. In the solid-state cross-polarization from ^{1}H to ^{13}C is an efficient technique for generating larger amounts of ^{13}C magnetization while taking advantage of the relaxation characteristics of the ^{1}H spin system (^{1}H $T_1 \approx 1$ s, a factor of 10−100 less than ^{13}C in the solid state). With such short proton relaxation times in the solid state, one can pulse every 2−3 s without any carbon saturation effects; here, the optimum S/N per unit time is obtained at a recycle delay of 1.25 ^{1}H T_1. A 4-fold higher carbon signal is also expected due to the higher proton polarization ($\gamma_H/\gamma_C = 4$). Finally, room or low temperature measurements gain higher equilibrium spin polarization (Boltzmann distribution), leading to 1.5× in signal enhancement (roughly 2× in measurement time). Notably this technique should not exploit NOEs that need calibration, and therefore it might be considered more robust than a melt measurement if simply the total number of CH_3 groups per molecule needs to be detected.

To realize the potential of these signal improvements via CP/MAS on semicrystalline PE, one must take into account the heterogeneous environment found in typical semicrystalline samples. At room temperature branched polyethylene carbon sites can be found in at least three structurally distinct regions—crystalline, interfacial, and amorphous regions—and consequently a dispersion in cross-polarization rates T_{CH} is observed. This generates a mismatch in the signal intensities between lattice-bound carbons and interfacial or amorphous carbons and hampers contact time optimization and therefore the capability of producing quantitative spectra. We suggest that the effects arising from spatial heterogeneity can be moderated to some extent by conducting a calibration at 253 K instead of room temperature. If the sample is cooled toward T_g, some conformational mobility is frozen out, and this helps to equalize the cross-polarization efficiency of amorphous carbons and crystalline carbons.

A contact time study was performed on sample B-16c at 298 and 253 K. The carbon magnetization transferred under Hartmann−Hahn (HH) conditions,[1] sampled as a function of the contact time, showed an initial buildup rate T_{CH} which was sensitive to the local carbon environment. Signal intensity at the crystalline carbons (32.7 ppm) reached a maximum at 400−600 μs contact time and was not affected by the temperature (<298 K) due to the relative low chain mobility within the crystallite at these temperatures.[38] Signal intensity at carbon 1 (≈14 ppm) reached a maximum at 2−4 ms contact time at room temperature but was shortened to 1−3 ms at 253 K. A contact time where the signal was close to a maximum for both signals was 1−1.2 ms. This value minimizes errors due to inefficient polarization transfer. Typical errors are estimated in the ±10% range.

In Figure 7, the ^{13}C spectra of the series of the 1-octene copolymers observed in the melt at 423 K are shown alongside the CP/MAS measurement obtained at 253 K. The branch contents determined in the solid-state measurement are in good agreement with the reference melt spectra, though systematically underestimated by ∼25%. The results of these investigations together with experimental parameters are listed in Table 4. The low temperature measurement using CP/MAS might be useful for rapid branch content determination or end-group analysis of samples with unknown thermal history. Room temperature CP/MAS measurement could also be applicable in favorable cases, for example, highly crystalline samples which have highly restricted chain mobility, or in cases where only relative changes within a series of samples are of interest.

Optimized Acquisition. In Figure 8, we display the results of the combined efforts toward sensitivity improvements explored within this article. Both (a) ^{13}C single pulse in the melt (423 K) and (b) CP/MAS below room temperature (253 K) were used to characterize a linear polyethylene with M_n = 114 000 g/mol, having only 1 CH_3 group per 4000 CH_2 groups. Spectra were taken using an optimized parameter set. The CH_3 resonance (carbon no. 1) is clearly visible in both spectra and shows a S/N of 3.6 for the melt and 7.9 for the solid-state CP/MAS. The acquisition time was less than 17 h for each spectrum; see Table 3 for details. Be aware of the 4000 times more intense peak at 30 ppm which clearly visualizes the achieved sensitivity. Peak integration gave an NMR-determined molecular weight within 20% relative accuracy of GPC-determined value: M_n(melt) = 122 800 g/mol (melt) and M_n(CP/MAS) = 134 400 g/mol.

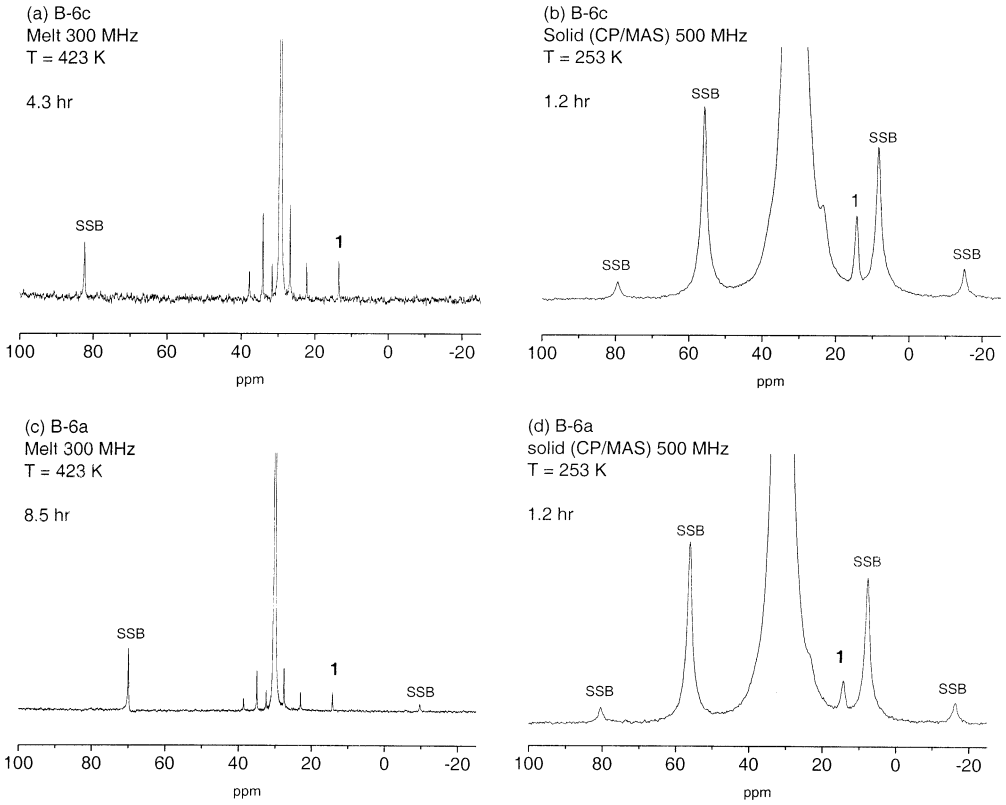

Figure 7. Comparison of the ^{13}C/MAS (melt) and ^{13}C CP/MAS (solid state) spectra obtained for two octene copolymers. See Table 4 for relevant parameters. From the reduced measurement time, the CP/MAS spectra indicate a high sensitivity toward chain branching using solid-state NMR techniques.

Table 4. Summary of Relevant Parameters for the Spectra Shown in Figure 7

Figure	7a	7b	not shown	not shown	7c	7d
sample	B-6c, melt	B-6c, solid	B-6b, melt	B-6b, solid	B-6a, melt	B-6a, solid
pulse seq	SPE/MAS	CP/MAS	SPE/MAS	CP/MAS	SPE/MAS	CP/MAS
instrument (MHz)	300	500	300	500	300	500
T (K)	423	253	423	253	423	253
no. of transients	512	2048	128	2048	256	2048
rec delay (s)	60	2	30	2	60	2
S/N	14.8	28.5	9.1	35.1	9.4	57.2
time (h)	8.5	1.2	1.1	1.2	4.3	1.2
branches/1000	12.4	8.9	7.6	5.3	4.73	3.4

Table 5. Tabulation of ^{13}C T_1 Spin−Lattice Relaxation Times, NOE Buildup Constants, and ^{13}C $T_{1\rho}$ Data Obtained for Several Different Polyethylene Architectures Measured at 423 K (Melt)

exp	label	* (methine)	alpha	beta	gamma	delta	1	2	3
^{13}C T_1 (s)	B-2	1.49 ± 0.08	1.11 ± 0.01	1.3 ± 0.01	1.24 ± 0.09	1.51 ± 0.03	6.31 ± 0.45	1.45 ± 0.05	
	B-6c	0.81 ± 0.04	0.65 ± 0.02	1.01 ± 0.05		1.48 ± 0.01	10.31 ± 0.83	7.75 ± 1.13	4.39 ± 0.62
	B-16c	0.71 ± 0.07	0.54 ± 0.02	0.98 ± 0.05		1.58 ± 0.04	9.77 ± 1.52	7.22 ± 0.82	4.69 ± 0.96
	B-26a	0.77 ± 0.21	0.67 ± 0.07	1.03 ± 0.07		1.92 ± 0.03	13.69 ± 1.29	8.68 ± 0.59	5.81 ± 0.5
	C-44					2.98 ± 0.07	13.8 ± 0.87	11.7 ± 0.61	8.71 ± 0.45
^{13}C NOE T_1 (s)	B-2	1.52 ± 0.07	1.11 ± 0.03	1.32 ± 0.03	1.42 ± 0.04	1.53 ± 0.01	7.03 ± 1.25	1.51 ± 0.05	
	B-6c	1.09 ± 0.14	0.84 ± 0.1	0.72 ± 0.06		1.77 ± 0.01	6.88 ± 6.04	6.76 ± 2.07	3.9 ± 0.34
	B-16c	0.45 ± 0.09	0.58 ± 0.04	1 ± 0.07		1.6 ± 0.03	22.1 ± 8.89	7.75 ± 1.51	7.32 ± 0.94
	C-44					2.71 ± 0.01	14.48 ± 0.87	12.2 ± 0.68	9.08 ± 0.28
^{13}C $T_{1\rho}$ (s)	B-2	0.27 ± 0.02	0.19 ± 0.01	0.19 ± 0.01	0.18 ± 0.01	0.13 ± 0.01			
	B-6c	0.15 ± 0.02	0.15 ± 0.01	0.22 ± 0.01		0.12 ± 0.01			
	B-16c	0.13 ± 0.02	0.145 ± 0.01	0.19 ± 0.01		0.15 ± 0.01			

In addition to the two end groups at 14 ppm, additional signals caused by α and β carbons are visible. Because of the fact that a single branch point generates three α and β carbons, we assume that about 50% are simply linear chains, but a certain fraction (≈50%) have a single branch point along the chain. Furthermore, it is interesting to recognize that resonances at 62, 71, and 73 ppm are visible. These resonances are attributed to oxygen present in the polymer chain. Because of the fact that the low-temperature CP/MAS spectrum was measured first, we conclude that the oxidization was already present in the polymer before measuring (perhaps from catalyst residues or the processing conditions); however, extended time-resolved measurements revealed a continuous increase in these signals as a function of time, indicating a tendency for this linear PE to oxidize during measurement. This tendency was not observed for the other polymers used in this study.

The result of Figure 8 shows that the end-group analysis is feasible for a 100 000 g/mol linear PE

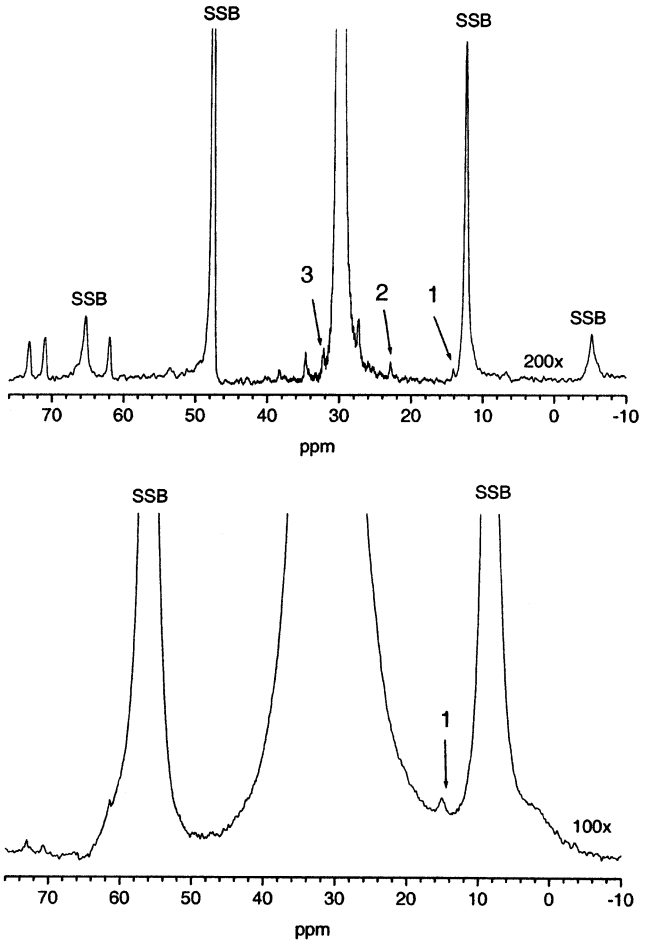

Figure 8. ^{13}C spectra of a linear standard PE (M_n = 114 000 g/mol) measured under optimized conditions using (a) SPE/MAS at 423 K (melt) and (b) CP/MAS at 253 K (solid state). Measurement time was 16.7 h for both spectra, with achievable S/N of 3.6 (SPE/MAS) and 7.9 (CP/MAS) on the methyl end carbon. The NMR determined M_n was 122 800 g/mol (SPE) and 134 400 g/mol (CP/MAS) (see Table 3). For this linear standard, it is worth noting that (a) branched structures could be detected (e.g., α peak at 34,5 ppm) and (b) small amounts of oxidation was determined via the peaks at 62, 71, and 73 ppm. Note that the CH_2 signal at 30 ppm is 4000 times as intense as the CH_3 signal at ~14 ppm.

	Method	Carbon Observed	Recycle Delay (sec)	S/N
1	Solution,SPE	*	60	10
2	Melt,SPE/MAS	*	60	10
3	Melt,SPE/MAS	*	10	10
4	Melt,SPE/MAS	*	2	10
5	Solid,CP/MAS	1	2	10
6	Melt,SPE/MAS	α	2	10
7	Melt,SPE/MAS	α	2	5

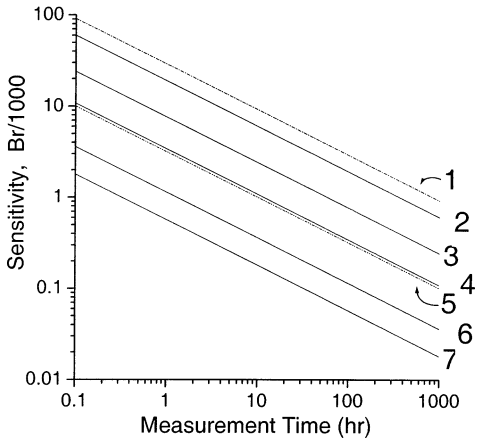

Figure 9. S/N analysis of several melt spectra obtained on linear and branched polyethylenes with variable measurement time using single-pulse excitation (SPE) and CP/MAS. This figure can be used a benchmark for the indicated S/N from a fully packed 7 mm rotor measured at 75 MHz ^{13}C resonance with the commercial solid-state MAS probe.

measured at 500 MHz within a single day using solid-state NMR. A severalfold improvement might still be achievable using even higher fields, specially optimized probes (e.g., increase in sample volume, $^1H-^{13}C$ optimized electronic circuits, cooling of signal transfer lines, improved power amplifiers, or decoupling schemes) or the addition of small amounts of relaxation agents such as $Cr(AcAc)_3$ in the melt. Investigations along these lines are currently being pursued in our laboratory.

We have summarized the results of solution-state, melt-state, and solid-state acquisitions of the model polyethylene copolymers in Figure 9. These lines express the sensitivity limits of these techinques for determining branch contents or end-group concentrations as a function of experimental time, measured at 300 MHz using 7 mm rotors. A vertical slice of the data through 24 h, for example, shows the expected sensitivity limit to be 1−2 branches per 10 000 backbone carbons when measured on the neat melt under the given conditions. Displayed in this format, the data emphasize how the choice of recycle delay and the desired S/N of a given carbon resonance are superimposed on the weak time dependence ($\sim t^{1/2}$). This figure should provide a reference point for further studies aimed at optimizing the measurements using either higher-field spectrometers, more robust probe designs, or other means. In addition to being a data summary, it should also provide some guidelines for choosing experimental parameters to achieve a given sensitivity.

Relaxation Parameters. Having achieved the maximum signal in a minimum amount of time, it was feasible to investigate the different spectroscopically resolved carbons toward the interrelation of branch length and relaxation parameters $T_{1\rho}$, T_1, and T_1^{NOE}. Because of the observations of the transient NOE, the relaxation times of the carbons in 1-butene, 1-octene, 1-octadecene, and 1-hexacosane copolymers have a direct influence on the signal proportionality and therefore will directly impact the determination of end-group and branch-point concentrations. In terms of detecting and quantifying long-chain branches, a crucial question is, at what side-chain length can we no longer distinguish a side-chain methyl group from a chain-end methyl group? In this context, it was of interest at the outset to determine these parameters as a basis to exploit a possible sensitivity to the branch length. The local melt dynamics are directly influenced by the local "defect" caused by the branched structure, at least for branches six carbons in length, but it is not known whether significantly longer branches have a significant effect on these parameters. A full list of evaluated relaxation times $T_{1\rho}$, T_1, and NOE buildup rates is given in Table 5.

Our first results (see Figure 10 and Table 5) on butene, octene, and higher branched copolymers in the melt for the ^{13}C relaxation parameters T_1, T_1^{NOE}, and $T_{1\rho}$ indicate a low sensitivity of $T_{1\rho}$ toward the side-chain length using all carbons that can be resolved in the spectra. On top of this, $T_{1\rho}$ can be very long in the melt

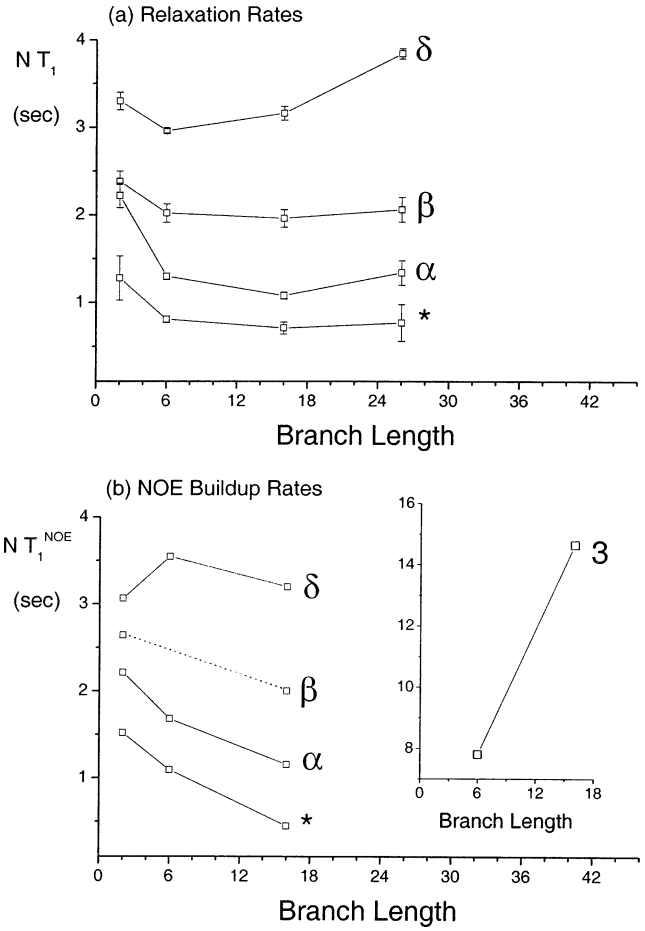

Figure 10. ^{13}C T_1s and selected T_1^{NOE} at 423 K (melt) for (a) side branch and (b) backbone carbons as a function of the side-chain branch length from $n = 2$ to $n = 28$. N refers to the number of covalent bound protons. Error bars indicate quality of fit, and guidelines are drawn between points.

(in the dimension of 100 ms) so that additional hardware problems are encountered. In contrast to the finding for $T_{1\rho}$, the variation of T_1 and T_1^{NOE} seems to have the best contrast for $n > 6$. This contrast is obviously a function of the side chain length and the carbons under investigation. To reduce measurement times, we focused on the faster relaxing backbone carbons. Figure 10a,b displays the ^{13}C T_1s and T_1^{NOE} build up rates as a function of the branch length, measured for the different comonomers at 300 MHz in the melt; error bars indicate the quality of fit, and lines are guide to the eyes. In the range where spectral resolution is still possible ($n = 6$), all the carbons display a dependence on the chain length except the bulk backbone carbons. This supports observations reported in the literature from the solution state and melt state.[9−12,14,23,24] Beyond $n = 6$, the T_1s of basically all carbons appear to have reached a plateau value for branch lengths between $n = 16$ and $n = 26$. The T_1 for the δ carbon seems to show the strongest correlation between side chain length and the relaxation rates. Within our first results, the T_1^{NOE} seems to extend the sensitivity toward longer branching the most. For the α carbon, this parameter is reduced by 50% from 1.11 to 0.58 s as the side-chain length is increased from $n = 2$ to $n = 16$. For carbon no. 3 T_1^{NOE} increases from 3.9 s ($n = 6$) to 7.3 s ($n = 16$).

It is not clear whether these results from model systems could be used, for example, to make a broad distinction between "shorter" long branches and "longer" long branches by examining the relaxation behavior for overlapping carbon resonances of an unknown sample. Further intense studies are needed to establish the limits for T_1 and T_1^{NOE} using longer side-chain model systems and to clarify whether such an approach would be fruitful. Higher B_0 field instruments could also be employed for signal improvements; however, one might observe a weak dependence of the carbon relaxation times as the field strength is increased, since not all carbons along the polyethylene chain are in the fast-motion limit. Any increase in the relaxation times would be most pronounced for the nuclei with the shortest relaxation times (e.g., the α carbon) and least pronounced for the longest (e.g., the methyl carbon).

Conclusions

We have shown that melt and solid-state ^{13}C/MAS measurements have high sensitivity toward the presence of sparsely branched side chains and end groups in polyethylene. Beyond a factor 10 in measurement time gained from moving from solution to the undiluted melt, sensitivity improvements were shown to be possible by exploiting the effects from transient NOEs by rapid pulsing. This allowed a further saving in measurement time by a factor of 3−8. However, the signal intensities observed under these conditions reflect a steady-state magnetization that gives an accurate branch content analysis only when comparing peak ratios for the methine, α, and β carbons to the bulk methylene signal. Accurate end-group analysis demands that recycle delays be in excess of 10 s, but solid-state CP/MAS measurements were shown to be a reasonable alternative for detecting methyl groups that avoids the transient NOE, despite the lowered spectral selectivity. Both the melt and solid-state approaches were successfully optimized so that M_n could be determined using end-group analysis for $M_n \sim 100\,000$ g/mol for PE in a 1 day measurement. NMR relaxation parameters $T_{1\rho}$, T_1, and T_1^{NOE} were evaluated for structures with 2, 4, 6, 16, and 26 side chain carbons in the melt. It was concluded that T_1^{NOE} for the α carbon and carbon no. 3 seems to be the most promising resonance for the evaluation of side chain branches with $n > 6$.

Acknowledgment. We would like to thank Dr. Hofe at Polymer Standards Service, Mainz for providing linear, narrow-distribution PEs, and Dr. Mirabella at Equistar, Cincinnati for providing a range of commercial PEs. M.P. and K.K. would also like to acknowledge stipends from the Max-Planck Society and Deutsche Forschungs Gemeinschaft (WI 1911/2-2), respectively.

References and Notes

(1) Schmidt-Rohr, K.; Spiess, H. W. *Multidimensional Solid-State NMR and Polymers*; Academic Press: London, 1994.
(2) Bovey, F. A.; Mirau, P. A. *NMR of Polymers*; Academic Press: San Diego, 1996.
(3) Komoroski, R. A., Ed.; *High-Resolution NMR Spectroscopy of Synthetic Polymers in Bulk*; VCH Publishers: Deerfield Beach, FL, 1986.
(4) Morris, G. A. Modern NMR Techniques for Structure Elucidation. *Magn. Reson. Chem.* **1986**, *24*, 371.
(5) Randall, J. C. A Review of High-Resolution Liquid C-13 Nuclear Magnetic Resonance Characterizations of Ethylene Based Polymers. *J. Macromol. Sci., Rev. Macromol. Chem. Phys.* **1989**, *C29*, 201.
(6) Yu, T. Y.; Guo, M. M. Recent Developments in C-13 Solid-State High-Resolution NMR of Polymers. *Prog. Polym. Sci.* **1990**, *15*, 825.

(7) Dais, P.; Spyros, A. C-13 Nuclear Magnetic Relaxation and local dynamics of synthetic polymers in dilute solution and in the bulk state. *Prog. Nucl. Magn. Reson. Spectrosc.* **1995**, *27*, 555 (Part 5-6).
(8) Shroff, R. N.; Mavridis, H. Assessment of NMR and Rheology for the Characterization of LCB in Essentially Linear Polyethylenes. *Macromolecules* **2001**, *34*, 7362.
(9) Komoroski, R. A.; Maxfield, J.; Mandelkern, L. C-13 Spin Relaxation Parameters of Completely Amorphous and Semicrystalline cis-Polyisoprene. *Macromolecules* **1977**, *10*, 545.
(10) Komoroski, R. A.; Maxfield, J.; Mandelkern, L. C-13 Spin Relaxation Parameters of Semicrystalline Polymers—Linear Polyethylene. *Macromolecules* **1977**, *10*, 550.
(11) Axelson, D.; Mandelkern, L.; Levy, G. C. C-13 Spin Relaxation Parameters of Branched Polyethylenes, Ramifications for Quantitative Analysis. *Macromolecules* **1977**, *10*, 557.
(12) Axelson, D. E.; Levy, G. C.; Mandelkern, L. Quantitative Analysis of Low Density (Branched) Polyethylenes by C-13 Fourier Transform Nuclear Magnetic Resonance at 67.9 MHz. *Macromolecules* **1979**, *12*, 41.
(13) VanderHart, D. L.; Garroway, A. N. C-13 rotating frame relaxation in a solid with strongly coupled protons: Polyethylene. *J. Chem. Phys.* **1979**, *71*, 2773.
(14) Cavagna, F. Distinction between Hexyl and Longer Branches in Polyethylene by 67.9 MHz C-13 NMR. *Macromolecules* **1981**, *14*, 215.
(15) Dechter, J. J.; Komoroski, R. A.; Axelson, D. E.; Mandelkern, L. C-13 NMR Linewidths of Polyethylenes and Related Polymers. *J. Polym. Sci., Polym. Phys.* **1981**, *19*, 631.
(16) Muller, G.; Schroder, E.; Chudzynski, L.; Wagnitz, U. Investigations on the branching of Chain Molecules. 23. Long-Chain Branching in Polyolefins—Comparison of the Results Obtained by C-13 NMR Spectroscopy and Investigation of Molecule Contraction in Solution. *Acta Polym.* **1983**, *34*, 345.
(17) Axelson, D. E.; Mandelkern, L.; Popli, R.; Mathieu, P. C-13 NMR of Polyethylenes—Correlation of the Crystalline Component T1 with Structure. *J. Polym. Sci., Polym. Phys.* **1983**, *21*, 2319.
(18) Usami, T.; Takayama, S. Fine-Branching Structure in High-Pressure, Low-Density Polyethylenes by 50.10 MHz C-13 NMR Analysis. *Macromolecules* **1984**, *17*, 1756.
(19) Freche, P.; Grenierloustalot, M. F. Characterization of Short Branches in a Low-Density Polyethylene by C-13 NMR. *Eur. Polym. J.* **1984**, *20*, 31.
(20) McFaddin, D. C.; Russell, K. E.; Kelusky, E. C. C-13 NMR solid state studies of relaxation behavior of branches in homogenous 1-alkene-ethylene copolymers. *Polym. Commun.* **1986**, *27*, 204.
(21) Bugada, D. C.; Rudin, A. Sizes of Long Branches in Low-Density Polyethylenes. *J. Appl. Polym. Sci.* **1987**, *33*, 87.
(22) Perez, E.; Bello, A.; Perena, J. M.; Benavente, R.; Martinez, M. C.; Aguilar, C. Solid-State Nuclear Magnetic Resonance Study of Linear Low-Density Polyethylenes. 1. Ethylene-1-Butene Copolymers. *Polymer* **1989**, *30*, 1508.
(23) de Pooter, M.; Smith, P. B.; Dohrer, K. K.; Bennett, K. F.; Meadows, M. D.; Smith, C. G.; Schouwenaars, H. P.; Geerards, R. A. Determination of the Composition of common Linear Low Density Polyethylene Copolymers by C-13 NMR Spectroscopy. *J. Appl. Polym. Sci.* **1991**, *42*, 399.
(24) Hatfield, G. R.; Killinger, W. E. Melt-State C-13 MAS NMR Determination of Comonomer Type and Content in Ethylene/a-Olefin Copolymers. *Anal. Chem.* **1995**, *67*, 3082.
(25) Hansen, E. W.; Blom, R.; Bade, O. M. NMR characterization of polyethylene emphasis on internal consistency of peak intensities and estimation of uncertainties in derived branch distribution numbers. *Polymer* **1997**, *38*, 4295.
(26) Liu, W.; Ray, D. G., III; Rinaldi, P. L. Resolution of Signal from Long-Chain Branching in Polyethylene by C-13 NMR at 188.6 MHz. *Macromolecules* **1999**, *32*, 3817.
(27) Wood-Adams, P. M.; Dealy, J. M.; deGroot, A. W.; Redwine, O. D. Effect of Molecular Structure on the Linear Viscoelastic Behavior of Polyethylene. *Macromolecules* **2000**, *33*, 7489.
(28) Alamo, R. G.; Blanco, J. A.; Carrilero, I.; Fu, R. Measurement of the C-13 spin-lattice relaxation time of the non-crystalline regions of semicrystalline polymers by a CP MAS-based method. *Polymer* **2002**, *43*, 1857.
(29) Litvinov, V. M.; Mathot, V. B. F. Partitioning of Main and Side-chain Units between Different Phases: A Solid-State C-13 NMR Inversion Recovery Cross-Polarization Study on a Homogeneous, Metallocene-Based Ethylene-1-Octene Copolymer. *Solid State Nucl. Magn. Reson.* **2002**, *22*, 218.
(30) *Metallocene-Based Polyolefins: Preparation, Properties, and Technology*; Schiers, J., Kaminsky, W., Eds.; Wiley: Chichester, 2000.
(31) Brintzinger, H.; Fischer, D.; Mülhaupt, R.; Rieger, B.; Waymouth, R. Stereospecific Olefin Polymerization with Chiral Metallocene Catalysts. *Angew. Chem., Int. Ed. Engl.* **1995**, *34*, 1143.
(32) Kaminsky, W.; Arndt, M. Metallocenes for Polymer Catalysis. *Adv. Polym. Sci.* **1997**, *127*, 145.
(33) Prasad, A. In *Polymer Data Handbook*; Mark, J., Ed.; Oxford University Press: Oxford, 1999; pp 529—539.
(34) Shroff, R.; Prasad, A.; Lee, C. Effect of molecular structure on rheological and crystallization properties of polyethylenes. *J. Polym. Sci., Polym. Phys.* **1996**, *34*, 2317.
(35) Qiu, X.; Ediger, M. D. Branching Effects on the Segmental Dynamics of Polyethylene Melts. *J. Polym. Sci., Polym. Phys.* **2000**, *38*, 2634.
(36) Qui, X.; Ediger, M. D. Local and Global Dynamics of Unentangled Polyethylene Melts by C-13 NMR. *Macromolecules* **2000**, *33*, 490.
(37) Okamoto, D. T.; Cooper, S. L.; Root, T. W. Control of Solid-State Nuclear Overhauser Enhancement in Polyurethane Block Copolymers. *Macromolecules* **1992**, *25*, 3301.
(38) Schmidt-Rohr, K.; Spiess, H. W. Chain Diffusion between Crystalline and Amorphous Regions in Polyethylene detected by 2-D Exchange C-13 NMR. *Macromolecules* **1991**, *24*, 5288.

MA0349130